

Broadband wavelength control for optical parametric oscillation in radially-poled whispering gallery resonators

Sarah-Katharina Meisenheimer^{a,b}, Josef U. Furst^a, Annelie Schiller^a, Karsten Buse^{a,b}, and Ingo Breunig^a

^aDepartment of Microsystems Engineering, University of Freiburg, Georges-Köhler-Allee 102, 79110 Freiburg, Germany

^bFraunhofer Institute for Physical Measurement Techniques IPM, Heidenhofstraße 8, 79110 Freiburg, Germany

ABSTRACT

Broadband infrared spectroscopy employing optical parametric oscillation in bow-tie cavities, including a periodically-poled lithium niobate (PPLN) crystal, is well known. We demonstrate, however, that such spectroscopy is also possible using 2-mm-size monolithic whispering gallery resonators (WGRs). This is achieved in a radially-poled WGR by controlling wavelength tuning despite triple resonance of pump, signal, and idler light. Simulated and measured tuning characteristics of the Type-0 OPOs, pumped at about 1 μm wavelength, coincide. Tuning branches, which are crossed or curved at degeneracy, are present over a spectral range of up to 0.9 μm . As a proof-of-principle experiment, we show that all spectroscopic features of ethanol can be resolved using the idler light between 2.2 and 2.55 μm .

Keywords: Whispering gallery resonator (WGR), nonlinear optics, parametric downconversion, optical parametric oscillation, periodic poling, quasi-phase-matching, spectroscopy

1. INTRODUCTION

Sources of infrared coherent light, which are tunable over a broad spectral range and having a narrow linewidth, are needed to perform spectroscopy of different molecules, e.g. in liquid mixtures. Singly-resonant Type-0 optical parametric oscillators (OPOs) pumped at about 1 μm are typically based on bow-tie cavities, which include a periodically-poled lithium niobate (PPLN) crystal. For these OPOs, all three light waves are extraordinarily polarized and the cavity resonantly enhances the power of the signal light. The tuning behavior of OPOs in bow-tie cavities can be theoretically described such that the output wavelengths are predictable.¹ Such OPOs are applicable to broadband infrared spectroscopy.²

Replacing the bow-tie cavity by a whispering gallery resonator (WGR) allows miniaturization of the system. These monolithic resonators are disk-shaped nonlinear-optical crystals that guide light by total internal reflection. Their diameter typically lies in the range between a couple of hundred micrometers and a few millimeters. Due to their high mechanical stability and their pump power thresholds in the microwatt range, they are well-suited for optical parametric oscillation.³ Continuous-wave operation and conversion efficiencies above 50 % have been demonstrated.⁴ Furthermore, narrowband spectroscopy using mode-hop-free tuning over 500 MHz has been shown.^{4,5} In order to achieve infrared Type-0 OPOs pumped around 1 μm in whispering gallery resonators, calligraphic poling of radial domain structures has been established.^{6,7}

However, matching simulations to measured tuning branches of Type-0 WGR-OPOs has not been possible up to now due to the variety of possible combinations of whispering gallery modes of the three waves interacting in the resonator. Furthermore, infrared spectroscopy over a wide spectral range using such WGR-OPOs is challenging.

In order to match simulations to experimental data, we study the tuning characteristics of Type-0 WGR-OPOs and present mode identification for pump, signal, and idler light. Pump mode identification in the

Corresponding author:

S.-K. Meisenheimer: E-mail: sarah.meisenheimer@imtek.uni-freiburg.de

transmission spectrum of a macroscopically-sized spheroidal resonator is achieved similar to the recipe of previous publications.^{8,9} In addition, for known pump modes, the OPO-tuning characteristics can be used to identify mode numbers of signal and idler light. Controlled wavelength tuning is presented despite triple resonance of pump, signal, and idler light. On the basis of these studies, broadband spectroscopy in the infrared spectral region using WGR-OPOs can be demonstrated.

The article is structured as follows: First, a calligraphically poled domain structure, the resonator fabrication and the experimental setup are presented. Subsequently, simulations of the tuning characteristics are shown and pump mode identification using spectral analysis is demonstrated. Based on these results, simulations of tuning branches can be fit to experimental data. This leads to the identification of the radial mode numbers of signal and idler light. Finally, the simulations are used to identify a tuning branch, which is suitable for broadband spectroscopy, such that ethanol can be spectroscopically investigated.

2. EXPERIMENTAL SETUP FOR WGR-OPOS

2.1 Fabrication of radially-poled whispering gallery resonators

Radial poling of near-stoichiometric lithium niobate doped with MgO (1.3 %) is achieved by calligraphic poling.^{6,7} Like for linearly-poled crystals used in bow-tie cavities, a period length of about 30 μm is needed to quasi-phase-match Type-0 OPOs pumped at around 1 μm . As a consequence, about 225 flipped domains are required for a resonator with 2 mm diameter. The poling structure of the resonator, used for the results presented in this article, is shown in Figure 1(a). We fabricate our resonators on a lathe using diamond pastes. By chemically etching the resonator, the domains can be visualized at the rim (see Fig. 1(b)). More details about our fabrication of radially-poled resonators can be found in a previous publication.⁷ The presented resonator has a major and a minor radius of about $R = 1.03$ mm and $r = 0.13$ mm, as measured by a white-light interferometer.

2.2 Experimental setup

The experimental setup for characterizing the OPO processes and identifying the mode numbers is sketched in Figure 1(c). We use an external-cavity diode laser (ECDL) with a wavelength of 1.0402 μm to pump the second-order nonlinear optical process. The mode-hop-free tuning range is 25 GHz and is monitored using a Fabry-Pérot interferometer (FPI). Extraordinarily polarized light is evanescently coupled from a single-mode fiber to the radially-poled WGR via a rutile prism. The signal and idler light is represented by the yellow and red lines. LP - low-pass filter, BS - beam splitter.

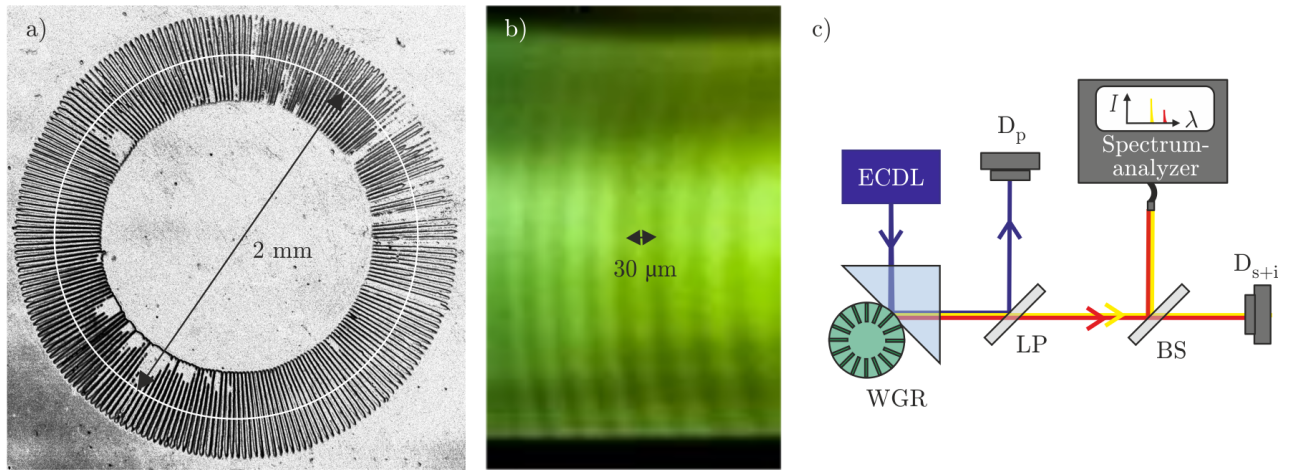


Figure 1. a) Radial poling structure in near-stoichiometric lithium niobate doped by MgO (1.3 %). The period length is about 30 μm . The white line indicates the rim of the future resonator with a diameter of about 2 mm. b) Resonator rim from side after fabricating the resonator and chemically etching it to visualize the poled domains. c) Sketch of the experimental setup used to characterize the optical parametric oscillation and to identify the mode numbers. The signal and idler light is represented by the yellow and red lines. LP - low-pass filter, BS - beam splitter.

The distance between resonator and prism is adjusted with the help of a piezoelectric actuator. A maximum coupling efficiency of about 40 % is reached at critical coupling. Furthermore, a temperature-stabilized oven and a housing ensure a millikelvin temperature stability of the resonator. The pump light and the generated light are separated by a low-pass filter and detected on D_p (silicon photodiode, absorbing up to 1.1 μm) and D_{s+i} (indium gallium arsenide, absorbing up to 2.55 μm), respectively. The wavelengths of the generated light are measured using an optical spectrum analyzer which is sensitive up to 2.55 μm and has an accuracy of 6 nm.

An intrinsic quality factor of 1.4×10^8 of the radially-poled resonator is deduced from 2 MHz linewidths in the pump spectrum. The quality factor of bulk lithium niobate measured at this wavelength is 1.5×10^8 .¹⁰ Obviously, surface roughness of the resonator plays a negligible role. Additionally, a minimal OPO threshold of about 20 μW is observed in undercoupling, whereas a maximum conversion efficiency of 45 % is attained in overcoupling.

3. BROADBAND WAVELENGTH TUNING

3.1 Simulation of the tuning behavior for multiple pump modes

In whispering gallery resonators, besides the fundamental mode (azimuthal, radial and polar pump mode numbers: $m \gg 1$, $q = 1$ and $p = 0$), higher modes with $q \geq 1$ and $p \geq 0$ occur for pump, signal, and idler light. As an example, Figure 2(a) shows the cross-section of the electric field distribution for a whispering gallery mode with $q = 3$ and $p = 1$.

The tuning behavior of whispering gallery resonators is simulated based on the theoretical description of eigenfunctions in whispering gallery resonators given by Gorodetsky's dispersion relation, phase-matching conditions and selection rules.^{3,11–13} The parameters for the simulations follow the experimental data (see Sec. 2.2): The refractive index is obtained by Gayer's Sellmeier equation for near-stoichiometric lithium niobate doped by MgO (1 %).¹⁴ The major and the minor radius of the WGR are 1.026 mm and 0.155 mm, respectively. Furthermore, a poling structure with $m_\Lambda = 225$ flipped domains is used. Optical parametric oscillation is pumped at 1.0402 μm wavelength.

If one mode number of the mode triplet of pump, signal, and idler changes, the output wavelength of optical parametric oscillation changes as well. Figure 2(b) demonstrates simulations of the tuning behavior of four equatorial pump modes ($p_p = 0$) with $q_p = 2, 3, 4$ and 5. These branches have the lowest threshold due to their strong mode overlap and therefore are expected to be most prominent in the experiment. The mode combinations are listed in Table 1.

As a consequence, instead of multiple grating periods used for bow-tie-OPOs, different mode combinations lead to various output wavelengths at fixed temperature. However, another feature is observable. Besides the

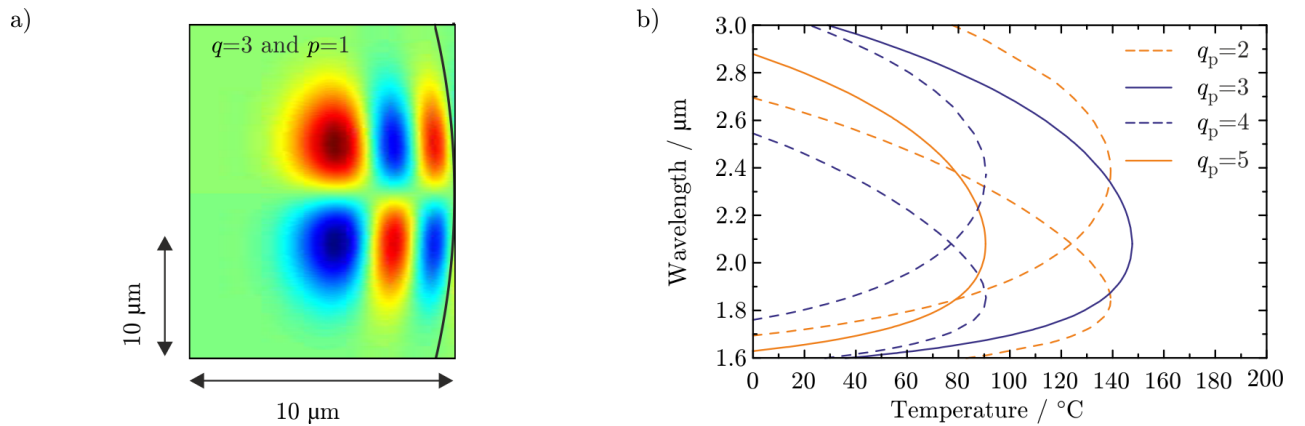


Figure 2. a) Cross-section of the electric field distribution for a mode with $q = 3$ and $p = 1$. b) Most prominent tuning branches of the equatorial pump modes $q_p = 2, 3, 4$ and 5 ($p_p = 0$ in all cases). For the mode numbers of signal and idler light, see Table 1.

Table 1. Mode numbers of pump, signal, and idler light for the tuning branches presented in Figure 2(b).

q_p	p_p	q_s	p_s	q_i	p_i
2	0	2	0	1	0
3	0	2	0	2	0
4	0	3	1	2	1
5	0	3	1	3	1

curved tuning branches ($q_p = 3$ and $q_p = 5$), which are known from Type-0 bow-tie OPOs, crossed tuning branches occur for $q_p = 2$ and $q_p = 4$ because here $q_s \neq q_i$. The spectral splitting of the tuning branches results from different effective refractive indices for the two mode combinations. In the case of bow-tie OPOs, crossed tuning branches are known from Type-II-OPOs for which the different effective refractive indices result from orthogonal polarizations of signal and idler light.¹⁵

3.2 Pump mode identification and control

The transmission spectrum of whispering gallery resonators can be simulated. According to the dispersion relation of spheroidal WGRs,¹¹ the frequency spacing between the resonances in the transmission spectrum, belonging to different modes, is given by the major and the minor radius of the resonator, the refractive index and the pump mode numbers. The major and the minor radius of the resonator and the pump wavelength (giving m_p) are experimentally determined (see Sec. 2.2). In addition, the refractive index of MgO-doped near-stoichiometric lithium niobate for extraordinary polarized light is given by Gayer's Sellmeier equation.¹⁴ As a consequence, q_p and p_p can be identified by fitting a simulated transmission spectrum to the measured data.

We focus our analysis on equatorial pump modes with $p_p = 0$, as higher p_p -modes are suppressed as shown in a previous publication.⁹ In contrast to previous publications,^{8,9} we present pump mode identification for a spheroidal radially-poled WGR made of near-stoichiometric lithium niobate without the need of an additional setup for emission patterns. This is achieved by analyzing the cross-correlation functions of experimental and simulated data. Figure 3 shows an experimental transmission spectrum measured at $T = 22^\circ\text{C}$. The radial mode numbers $q_p = 1 - 10$, as well as their position in the simulated spectrum (short black lines), are indicated. This match of simulations and experimental data is obtained for $\lambda_p = 1.041 \mu\text{m}$ and $R = 1.033 \text{ mm}$.

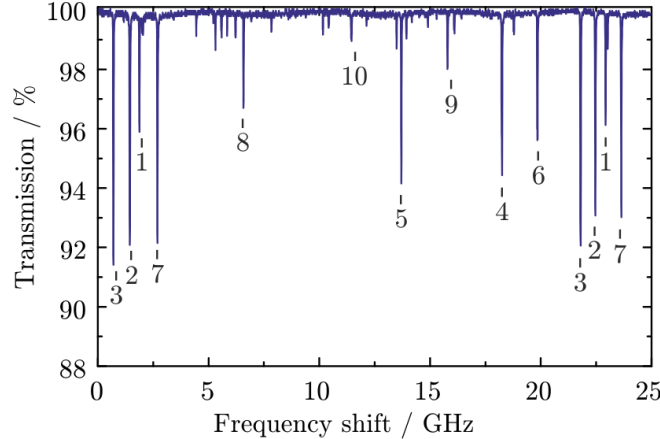


Figure 3. Identification of equatorial pump modes $q_p = 1 - 10$ in the transmission spectrum.

3.3 Comparison of measured and simulated tuning branches

Temperature-controlled wavelength tuning over a wide spectral range is achieved in two stages: q_p and p_p are kept fixed, and the corresponding pump resonance is tracked while changing the temperature. When increasing the pump power from below the pump power threshold, first, optical parametric oscillation for the tuning branch with the lowest pump power threshold is obtained. This tuning using pump mode control is explained in more detail in our previous publication.⁷ However, controlled broadband tuning also requires finding the tuning branch which has the lowest threshold over a spectral range that is as broad as possible. In order to locate the temperature range of such a tuning branch for a given pump mode, matching simulations of tuning branches to experimental data is essential. This additionally leads to mode identification for signal and idler light.

The most prominent simulated tuning branches for the equatorial modes with $q_p = 4$ and $q_p = 5$ have been presented in Section 3.1. They are applied as an indication for experiments. Figure 4 shows the experimental data of this crossed ($q_p = 4$) and this curved tuning branch ($q_p = 5$). The tuning branches are pursued over 65 °C and 45 °C and cover a spectral range of about 1.8 – 2.4 μm and 1.7 – 2.6 μm, respectively. The measurement is performed in 2 °C steps. For higher temperatures, the tuning branch presented in Figure 4(a) can not be followed anymore because another tuning branch has a lower threshold in that range. The same applies for the curved tuning branch at temperatures below 48 °C (see Figure 4(b)). Idler wavelengths above 2.55 μm are derived from the signal wavelength as they can not be detected using InGaAs-photodiodes (unfilled circles in Figure 4(b)).

Although WGR-OPOs are triply resonant, the linewidths of the resonances allow detunings from perfect resonance.^{16,17} A detuning from the pump resonance is indicated by an asymmetric pump resonance in the transmission spectrum. In this case, the pump power threshold rises. By using pump powers above the threshold and sweeping the laser over the resonance, optical parametric oscillation is obtained, even if triple resonance is not fulfilled. The presented experiments are performed in overcoupling. In this case, the linewidth below the OPO-threshold is about 20 MHz. Optical parametric oscillation is pumped by up to a factor of four above the power threshold ($4 P_{th}$), at which power the maximum efficiency is reached. Several OPO processes broaden the resonances up to 200 MHz. The pump laser, which is tunable over more than 25 GHz, is swept over the resonance. As a result of the allowed detuning, the two tuning branches are measurable at nearly all temperatures in the presented range.

By comparing the data to simulations, the radial mode numbers $q_s = 3$, $q_i = 2$ (for $q_p = 4$) and $q_s = 3$, $q_i = 3$ (for $q_p = 5$) are identified. The polar mode numbers fulfill $p_s + p_i = 2$ in both cases. The tuning branches with

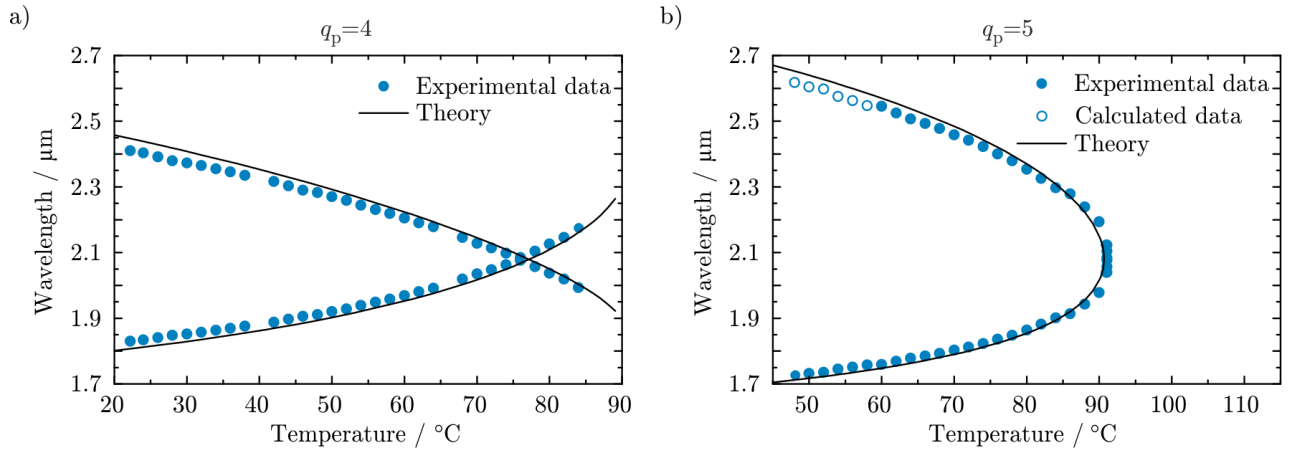


Figure 4. Crossed (a) and curved (b) tuning branches belonging to $q_p = 4$ and $q_p = 5$, respectively. The theoretical tuning branches obtained using simulations are fits to the experimental data. Thereby, the radial mode numbers $q_s = 3$, $q_i = 2$ (for $q_p = 4$) and $q_s = 3$, $q_i = 3$ (for $q_p = 5$), as well as $p_s + p_i = 2$ (for both cases), are identified. The unfilled circles indicate idler wavelengths calculated using the measured signal wavelength and energy conservation.

$p_s = p_i = 1$ have the lowest threshold and are shown in Figure 4. The good accordance of experimental and simulated data is achieved by adapting the major and the minor radius applied in the simulations.

4. APPLICATION: BROADBAND SPECTROSCOPY

The setup presented in Section 2.2 is extended for spectroscopy (see Fig. 5(a)). A second beam splitter and a reference arm with an indium gallium arsenide photodiode D_{ref} are added. According to the results from Section 3.3, the idler light of the curved tuning branch is used to demonstrate broadband spectroscopy between 2.2 and 2.55 μm of ethanol filled into a cuvette with 1 mm pathlength (see Fig. 5(b)). For spectroscopy, the OPO is temperature tuned in steps of 1 $^{\circ}\text{C}$. The measured data points exhibit very good accordance with the spectrum measured by a commercial photospectrometer (Varian Cary 500).

At large idler wavelengths, we are limited by the indium gallium arsenide photodiode. At low idler wavelengths, the slope of the curved tuning branch is very steep. Therefore, a crossed tuning branch with a smaller slope is more appropriate for spectroscopy between 2.1 and 2.2 μm .

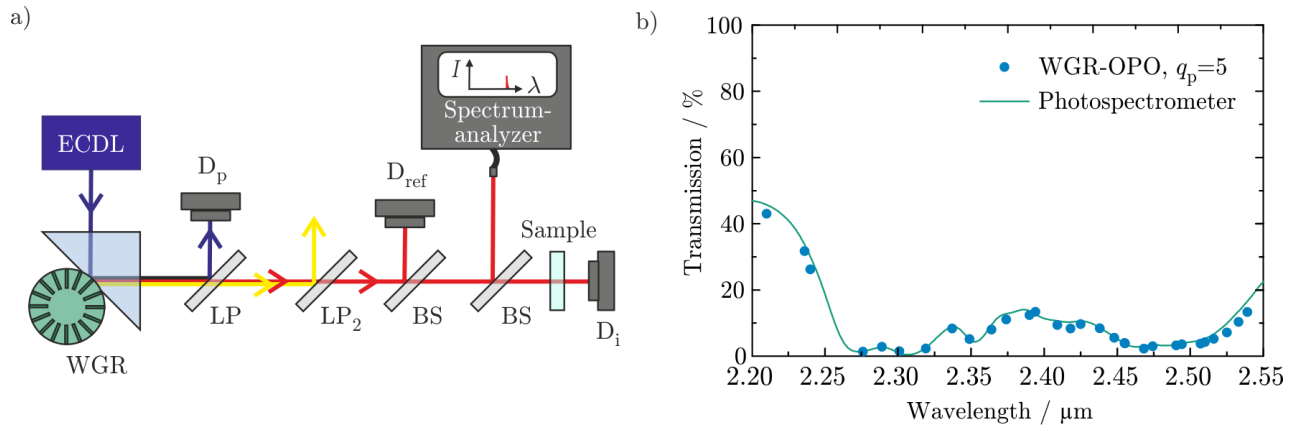


Figure 5. a) Experimental setup for spectroscopy using the idler light of WGR-OPOs (red line). A second low-pass filter and a reference arm are added in comparison to the setup used for characterization of the tuning branches (see Sec. 2.2). b) Spectroscopy of ethanol filled into a cuvette with 1 mm pathlength using the curved tuning branch (see Fig 4) in 1 $^{\circ}\text{C}$ steps and a photospectrometer (Varian Cary 500). The higher the wavelength, the smaller is the distance of the measurement points in x -direction due to the steeper slope of the curved tuning branch.

5. CONCLUSION

In this article, we have presented a radially-poled whispering gallery resonator applicable to Type-0 optical parametric oscillation. Simulations of tuning characteristics, controlled wavelength tuning over a broad spectral range and the identification of pump, signal, and idler modes have been achieved. Additionally, crossed and curved tuning branches have been demonstrated. We use the knowledge of the tuning branches to demonstrate spectroscopy of ethanol between 2.2 and 2.55 μm . Combined with narrowband wavelength-tuning,⁵ the presented broadband infrared spectroscopy paves the way for spectroscopy of demanding samples, such as gas mixtures, using one compact light source.

ACKNOWLEDGMENTS

The authors kindly acknowledge the Deutsche Forschungsgemeinschaft and the Deutsche Telekom Stiftung for financial support.

REFERENCES

- [1] Giordmaine, J. A. and Miller, R. C., “Tunable coherent parametric oscillation in LiNbO_3 at optical frequencies,” *Phys. Rev. Lett.* **14**(24), 973–976 (1965).
- [2] Arslanov, D. D., Spunoi, M., Mandon, J., Cristescu, S. M., Persijn, S. T., and Harren, F. J. M., “Continuous-wave optical parametric oscillator based infrared spectroscopy for sensitive molecular gas sensing,” *Laser & Photon. Rev.* **7**(2), 188–206 (2013).
- [3] Füst, J. U., Strekalov, D. V., Elser, D., Aiello, A., Andersen, U. L., Marquardt, C., and Leuchs, G., “Low-threshold optical parametric oscillations in a whispering gallery mode resonator,” *Phys. Rev. Lett.* **105**(26), 263904 (2010).
- [4] Werner, C. S., Buse, K., and Breunig, I., “Continuous-wave whispering-gallery optical parametric oscillator for high-resolution spectroscopy,” *Opt. Lett.* **40**(5), 772–775 (2015).
- [5] Schunk, G., Vogl, U., Strekalov, D. V., Förtsch, M., Sedlmeir, F., Schwefel, H. G. L., Göbelt, M., Christiansen, S., Leuchs, G., and Marquardt, C., “Interfacing transitions of different alkali atoms and telecom bands using one narrowband photon pair source,” *Optica* **2**(9), 773–778 (2015).
- [6] Mohageg, M., Strekalov, D. V., Savchenkov, A. A., Matsko, A. B., Ilchenko, V. S., and Maleki, L., “Calligraphic poling of lithium niobate,” *Opt. Express* **13**(9), 3408–3419 (2005).
- [7] Meisenheimer, S.-K., Füst, J. U., Werner, C., Beckmann, T., Buse, K., and Breunig, I., “Broadband infrared spectroscopy using optical parametric oscillation in a radially-poled whispering gallery resonator,” *Opt. Express* **23**(18), 24042–24047 (2015).
- [8] Schiller, S. and Byer, R. L., “High-resolution spectroscopy of whispering gallery modes in large dielectric spheres,” *Optics Letters* **16**(15), 1138–1140 (1991).
- [9] Schunk, G., Füst, J. U., Förtsch, M., Strekalov, D. V., Vogl, U., Sedlmeir, F., Schwefel, H. G. L., Leuchs, G., and Marquardt, C., “Identifying modes of large whispering-gallery mode resonators from the spectrum and emission pattern,” *Opt. Express* **22**(25), 30795–30806 (2014).
- [10] Leidinger, M., Fieberg, S., Waasem, N., Kühnemann, F., Buse, K., and Breunig, I., “Comparative study on three highly sensitive absorption measurement techniques characterizing lithium niobate over its entire transparent spectral range,” *Opt. Express* **23**(17), 21690–21705 (2015).
- [11] Gorodetsky, M. L. and Fomin, A. E., “Geometrical theory of whispering-gallery modes,” *IEEE J. Select. Topics Quantum Electron.* **12**(1), 33–39 (2006).
- [12] Breunig, I., Sturman, B., Sedlmeir, F., Schwefel, H. G. L., and Buse, K., “Whispering gallery modes at the rim of an axisymmetric optical resonator: Analytical versus numerical description and comparison with experiment,” *Opt. Express* **21**(25), 30683–30692 (2013).
- [13] Matsko, A. B., Ilchenko, V. S., Savchenkov, A. A., and Maleki, L., “Highly nondegenerate all-resonant optical parametric oscillator,” *Phys. Rev. A* **66**(4), 043814 (2002).
- [14] Gayer, O., Sacks, Z., Galun, E., and Arie, A., “Temperature and wavelength dependent refractive index equations for MgO-doped congruent and stoichiometric LiNbO_3 ,” *Appl. Phys. B* **91**(2), 343–348 (2008).
- [15] Vodopyanov, K. L., “Optical THz-wave generation with periodically-inverted GaAs,” *Laser & Photon. Rev.* **2**(1-2), 11–25 (2008).
- [16] Sturman, B., Beckmann, T., and Breunig, I., “Quasi-resonant and quasi-phase-matched nonlinear second-order phenomena in whispering-gallery resonators,” *J. Opt. Soc. Am. B* **29**(11), 3087–3095 (2012).
- [17] Breunig, I., Sturman, B., Bückle, A., Werner, C. S., and Buse, K., “Structure of pump resonances during optical parametric oscillation in whispering gallery resonators,” *Opt. Lett.* **38**(17), 3316–3318 (2013).